Cretaceous Research 164 (2024) 105953

Contents lists available at ScienceDirect

Cretaceous Research

journal homepage: www.elsevier.com/locate/CretRes

Palynology of the Albian–Turonian sediments from the Sumbe region, Kwanza Basin (Angola): Implications for paleoenvironment, paleoclimate, and paleogeography

Cristina Rodrigues [a, b], Márcia Mendes [c, *], Zélia Pereira [c], Pedro Claude Nsungani [d], Paulo Fernandes [e], Luís Vítor Duarte [f], Belarmino Chitangueleca [g], Lúmen Sebastião [g], Benedito Aida [g], Davide Degli Esposti [h], Domingos Freitas [i]

[a] FP-ENAS, Universidade Fernando Pessoa, Praça de 9 de Abril, 349, Porto 4249-004, Portugal
[b] MARE – Centro de Ciência do Mar e Ambiente/URI Coimbra, Portugal
[c] LNEG, Rua da Amieira, S. Mamede de Infesta, 4465-965, Portugal
[d] Departamento de Geologia, Faculdade de Ciências, Universidade Agostinho Neto, Avenida 4 de Fevereiro, 71, Luanda, Angola
[e] CIMA, Centre of Marine and Environmental Research|ARNE – Infrastructure Network in Aquatic Research, University of Algarve, Campus de Gambelas, Faro 8000-139, Portugal
[f] Universidade de Coimbra, MARE-ARNET e Departamento de Ciências da Terra, Coimbra, Portugal
[g] Exploration Division (DEX) – Agência Nacional de Petróleo, Gás e Biocombustíveis (ANPG), Luanda, Angola
[h] PGS Geophysical Angola, Angola
[i] Geoscience Division – Victory Oil and Energy (VOE), Angola

A R T I C L E I N F O

Article history:
Received 3 January 2024
Received in revised form
13 June 2024
Accepted in revised form 13 June 2024
Available online 1 July 2024

Keywords:
Albian–Turonian
Dinoflagellate cysts
Sporomorphs
South atlantic
Gondwana breakup

A B S T R A C T

Palynological investigations in the Sumbe region of the Kwanza Basin, Angola, have identified Albian to Turonian assemblages in four sections of the Quissonde Facies of the Mucanzo, Cabo Ledo, and Itombe formations. These studies aimed to determine their biostratigraphic ages and infer paleoenvironmental, paleoclimatic, and paleogeographic models. The presence of *Odontochitina costata, Palaeohystrichophora infusorioides,* and *Xiphophoridium alatum* cysts supports an upper Albian to lower Cenomanian age for the Mucanzo Formation. *Litosphaeridium siphoniphorum* cyst and the *Elateroplicites africaensis* pollen found In the Cabo Ledo Formation suggest a Cenomanian age, while *Conosphaeridium striatoconum, Heterosphaeridium difficile,* and *Dinogymnium acuminatum* supports a Turonian age for the lower part of the Itombe Formation. All samples predominantly contain fluorescent amorphous organic matter (AOM) derived from phytoplankton degradation, with increasing AOM in the uppermost units, indicating inner neritic marine deposition under dysoxic-anoxic conditions. During the Lower to mid-Cretaceous, the Gondwana breakup caused significant changes, with the palynological indicating a Tethyan affinity with some high-latitude taxa, suggesting a cosmopolitan distribution. The subtropical to tropical nature of the assemblages, along with high-latitude species, indicates a mid-Cretaceous water connection between the Central Atlantic and the South Atlantic oceans, extending to the Kwanza Basin.

1. Introduction

The Cretaceous was primarily characterized by a warm climate attributed to increased volcanic-derived carbon dioxide emissions, creating greenhouse conditions (*e.g* Barron et al., 1981; Chumakov et al., 1995; Clarke and Jenkyns 1999; Föllmi 2012; Friedrich et al., 2012; Bodin et al., 2015; O'Brien et al., 2017). Consequently, significant periods of oceanic anoxic conditions occurred during this time, leading to the accumulation of organic-rich sediments crucial for the hydrocarbon industry. Despite limited studies on biostratigraphy in the Kwanza Basin, some authors have addressed the mid-

* Corresponding author.
E-mail addresses: cfrodrig@gmail.com (C. Rodrigues), marcia.mendes@lneg.pt (M. Mendes), zelia.pereira@lneg.pt (Z. Pereira), pedroclaudensungani@yahoo.com.br (P.C. Nsungani), pfernandes@ualg.pt (P. Fernandes), belarmino.Chitangueleca@anpg.co.ao (B. Chitangueleca), Lumen.Sebastiao@anpg.co.ao (L. Sebastião), benedito.aida@anpg.co.ao (B. Aida), davide.Degli.Esposti@pgs.com (D.D. Esposti), dgmanager@victoryoe.com (D. Freitas).

https://doi.org/10.1016/j.cretres.2024.105953

Cretaceous. The Quissonde Facies of Mucanzo Formation and Cabo Ledo Formation, characterized by carbonate-siliciclastic facies, contain pelagic foraminifera indicative of the upper Albian and Cenomanian, respectively (Meijer, 1989; Morais et al., 1990). Similarly, the Itombe Formation, based on echinoderm taxa, is assigned to the Upper Cretaceous (Haughton, 1924; Kier and Lawson, 1978; Néraudeau and Mathey, 2000). Furthermore, biostratigraphic studies conducted on foraminifers and nannoplankton in the Angola Continental Margin by Bruno et al. (2020) and Magniez-Jannin and Muller (1987) suggest an Albian–Cenomanian age for the studied section, although lithostratigraphic correlation remains unclear.

Thus, this study aims to palynologically analyze the Quissonde Facies of Mucanzo, Cabo Ledo, and Itombe formations in the Sumbe region of the Kwanza Basin (Fig. 1) to (1) confirm palynological ages and correlate them with previously established ages based on other fossils and (2) characterize the depositional paleoenvironments.

2. Geological setting

The Kwanza Basin is one of the classic passive margin basins on the West African margin that developed due to the Gondwanaland rifting. This rift-to-drift margin evolved as a product of the separation of South America and Africa, leading to the opening of the South Atlantic Ocean (Brognon and Verrier, 1966; Guiraud et al., 2010; Moulin et al., 2010; Serié et al., 2017)The study area (Sumbe) (Fig. 2) lies near the coast in the southern portion of the Kwanza Basin (Buta-Neto et al., 2006; Quesne et al., 2009; Guiraud et al., 2010).

The general stratigraphic column of the Kwanza Basin (as per Brognon and Verrier, 1966; Total-Sonangol, 1987; Brownfield and Charpentier, 2006; Guiraud et al., 2010; Fig. 2) begins with a pre-rift megasequence (Jurassic-Lower Cretaceous?) represented by terrigenous detrital deposits, indicative of continental-alluvial, fluvial, and lacustrine environments. Following this, a syn-rift megasequence (Lower Cretaceous, Barremian to lower Aptian?) unfolds, featuring fluvial deposits consisting of conglomerates and coarse-grained sandstones (Red Cuvo Formation), alongside lacustrine deposits like shales, organic-rich shales, fine-grained sandstones, and siltstones (Grey Cuvo Formation). This phase culminates with conglomerates, red sandstone, claystone, and dolomite from transitional environments (Cuvo and Chela formations), which represent the end of rifting. Subsequently, the post-rift megasequence (upper Aptian to present-day) was initially (during the

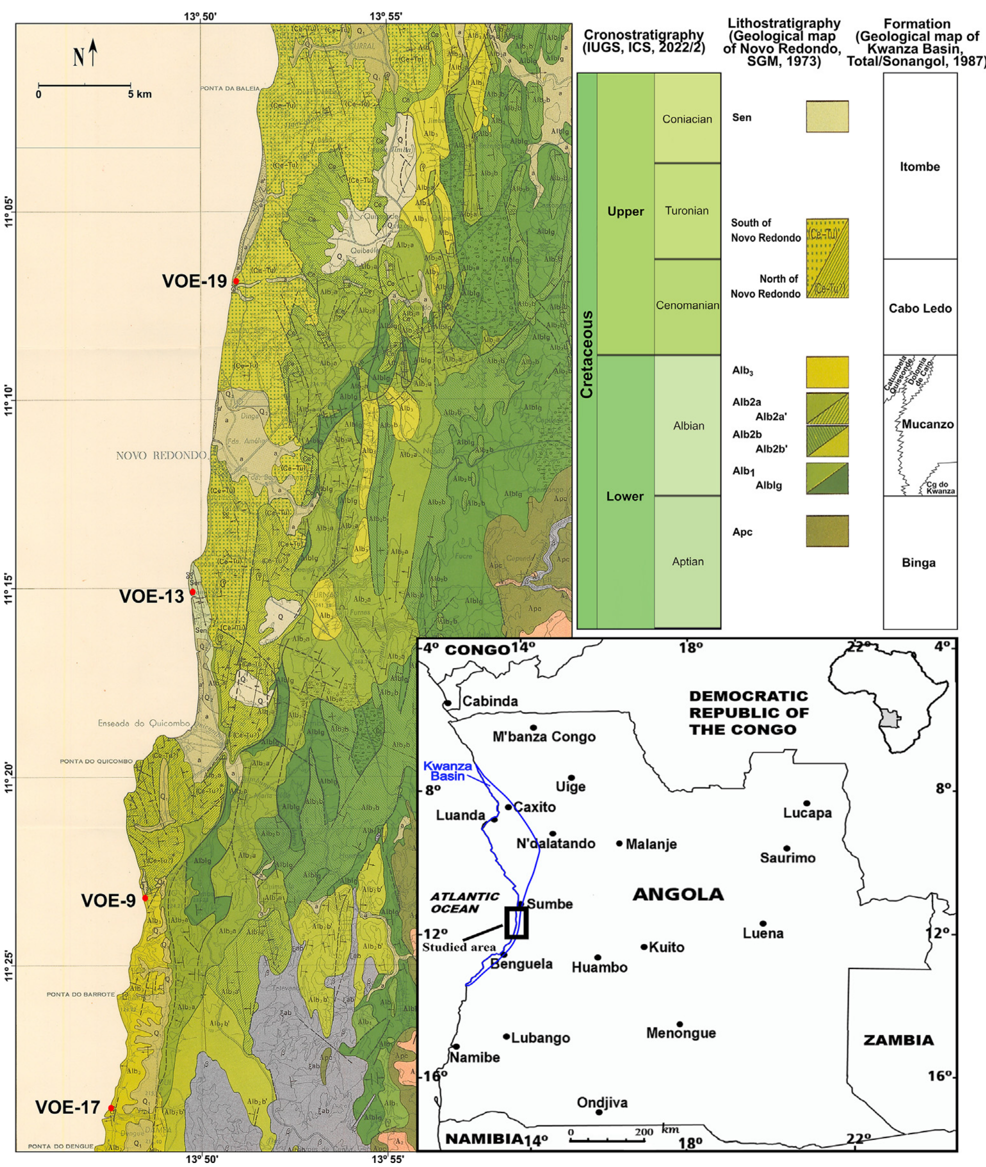

Fig. 1. Geological map of the studied area (Lapão and Simão, 1973).

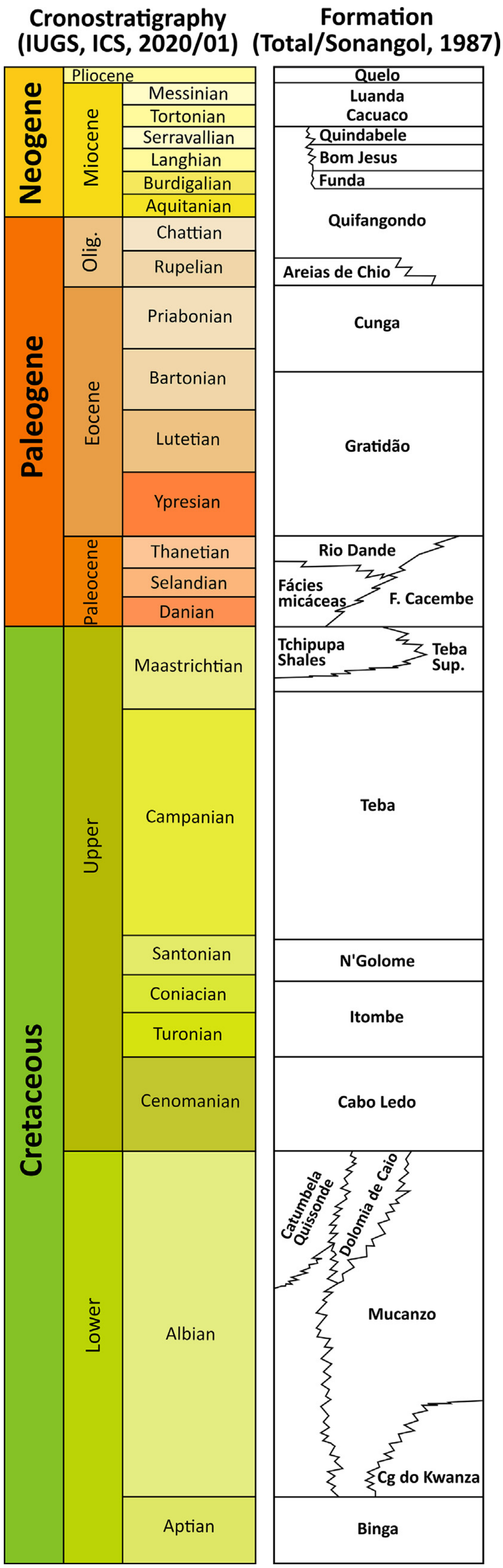

Fig. 2. The chronostratigraphic sequence of Kwanza Basin (Lapão and Simão, 1973).

Albian to Eocene age) defined by a regional transgressive setting, transitioning into a regional regressive regime from the Oligocene to the present. The Binga Formation (upper Aptian to Albian) represents the first marine transgressive deposits, and accommodating a carbonate sequence within a marine-lagoonal environment. This formation is succeeded by carbonate-evaporite cycles from the Albian (Mucanzo Formation). From the Cenomanian to Maastrichtian (Late Cretaceous), widespread organic-rich marine shales, siltstones, and marls (Cabo Ledo, Itombe, N'Golombe, and Teba formations) developed laterally and above the carbonate units.

The stratigraphic sequence and ages of the Cretaceous marine formations of the Kwanza Basin, especially its southern portion (Carvalho, 1961; Cooper, 2003a, 2003b), remain controversial and poorly defined, largely due to the absence of distinct lithostratigraphic markers.

Progradational marine conditions dominated the Cenozoic units. The Paleocene (Rio Dande Formation) and Eocene to Oligocene (Cunga and Gratidão formations) consist of sandstones and siltstones, turbidites, and deep-marine deposits. During the Miocene (Quifangondo Formation), the marine conditions persisted, with deposits mainly comprising poorly sorted materials and locally channel-filled sandstones and turbidites. The Pliocene and Pleistocene are represented by a detrital sequence (Luanda Formation).

3. Studied sections

The Sumbe region of the Kwanza Basin is renowned for its well-exposed Upper Cretaceous units, with a 40 km long section along the southern Kwanza Basin coast (Fig. 1). According to the Geological Map of "Novo Redondo" (Lapão and Simão, 1973), the Sumbe section encompasses the Binga Formation, Quissonde Facies of the Mucanzo Formation (following Total-Sonangol, 1987), Cabo Ledo and Itombe formations. Fig. 3 and Table S1 outline the lithologies and positions of the palynological samples analyzed.

Section VOE-17, identified in accordance with the Geological Map of "Novo Redondo" (Lapão and Simão, 1973) and Total-Sonangol (1987), represents the Quissonde Facies of the Mucanzo Formation, dated to the upper Albian in age. The lower segment (samples VOE-17A and VOE-17B, Fig. 3) comprises an interval of approximately 5 m thick, represented by grey and yellowish marlstone interbedded by limestone. Some of the limestone beds are dolomitic limestones. The upper portion (samples VOE-17C and VOE-17D, Fig. 3) is approximately 40 m thick, characterized by marlstones, conglomerates, and medium- to coarse-grained sandstones. This sequence has several characteristics that confirm the existence of a channel. The conglomerate package is cutting the underlying marlstones, creating an erosional surface. Conglomerates at the bottom rise to medium-grained sandstones at the top, producing the graded bedding representing the channel filling. A 15 cm thick claystone layer separates the two packages.

Section VOE-9, located approximately 12 km north of section VOE-17 (Fig. 1), also corresponds to the Quissonde Facies of the Mucanzo Formation (following Lapão and Simão, 1973; Total-Sonangol, 1987)) of the upper Albian. It features a 6 m thick interval containing conglomeratic coarse-grained sandstone, medium-grained sandstone, and claystone (samples VOE-9A, VOE-9B, VOE-C, and VOE-9D, Fig. 3). The conglomeratic coarse-grained sandstone package cuts into the claystone through an erosional surface, forming a filling channel. Additionally, conglomeratic coarse-grained sandstones are onlapping the channel sides, and the

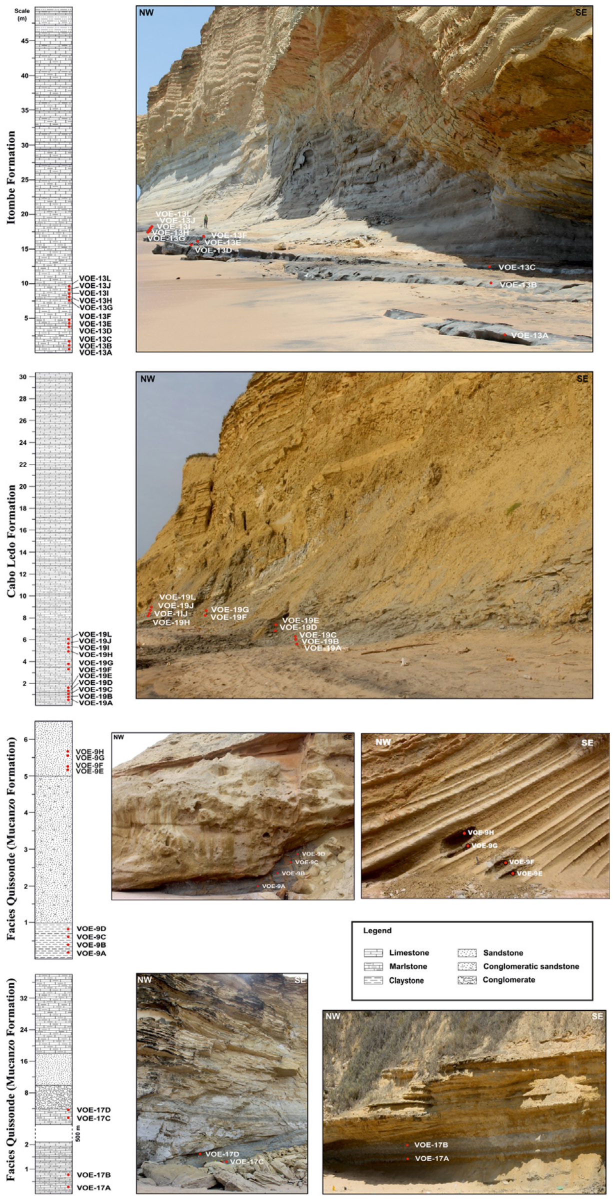

Fig. 3. Sumbe region selected sections, presenting lithologies and position of the productive palynological samples analyzed.

sequence exhibits changes in grain size toward the top, indicating shallowing up to the surface.

Section VOE-19, located approximately 32 km north of VOE-9 (Fig. 1), is about 30 m thick and is characterized by black and grey marlstones (samples VOE-19A, VOE-19B, VOE-19C, VOE-19D, VOE-19E, VOE-19F, VOE-19G, VOE-19H, VOE-19I, VOE-19J, and VOE-19L, Fig. 3) interbedded by limestones from the Cabo Ledo Formation (following Total and Sonangol, 1987), assigned to the Cenomanian and Turonian, according to the Geological Map of “Novo Redondo” (Lapão and Simão, 1973). Carbonate deposits increase towards the top of the section.

Section VOE-13, located near Sumbe city and about 17 km south of VOE-19 (Fig. 1), correlates with the Itombe Formation (Lapão and Simão, 1973), tentatively dated to the Coniacian (Total-Sonangol, 1987). This section, approximately 50 m thick, comprises black and grey marlstone (samples VOE-13A, VOE-13B, VOE-13C, VOE-13D, VOE-13E, VOE-13F, VOE-13G, VOE-13H, VOE-13I, VOE-13J, and VOE-13L, Fig. 2), limestone and sandstone (Fig. 2), with an increase in silty sediments towards the top and laminated black marlstone beds. *Planolites* and ammonites are common in these pelagic limestones, suggesting open sea conditions, meaning distal shelf deposition.

4. Methods

Palynostratigraphic and palynofacies (organic facies) studies were conducted at the National Laboratory of Energy and Geology (Portugal), following standard procedures to extract and concentrate the organic matter (Wood et al., 1996; Riding and Warny, 2008). Initially, all samples (ca. 50 g of rock) underwent treatment with HCl (37%) and HF (48%) to remove carbonate and silicate minerals. The resulting residues were sieved using a 20 μm opening sieve, and the organic residues were stained with safranin-O to enhance morphological features visibility. Subsequently, the organic residues were mounted on microscope slides using a resin-based mounting medium (*e.g.,* Entelan®) and examined under transmitted light using a Nikon eclipse Ci microscope. All samples, residues, and slides are archived in the Palynological Collection of the Geological Survey of Portugal, LNEG, S. Mamede de Infesta (Portugal).

Out of 34 samples investigated, 19 samples were considered palynologically productive (Table S1) and suitable for quantitative and qualitative palynological analysis, based on the key-palynomorph distribution (Table S2, Fig. 4) focusing on the lowest and the highest occurrences. A quantitative assessment was performed by counting a minimum of 150 palynomorphs per sample and grouped into the major classes: i) spores, ii) pollen, iii) fungal remains, iv) dinoflagellate cysts (dinocysts; gonyaulacales and peridiniales), v) microforaminiferal linings, scolecodonts and, vi) other aquatic palynomorphs (Table S2). However, a few samples, such as VOE-13C and VOE-13H did not meet this count due to the low diversity and poor preservation of the palynomorphs. The nomenclature of dinocysts cyst species and suprageneric classification follows (Fensome et al., 2008, 1993), and descriptive morphological terminology is based on (Williams et al., 2017a; 2017b).

For assessing the depositional environment, 29 samples were considered productive (Table S2). During this analysis, the identification and general description of the organic components of phytoclasts, palynomorphs, and amorphous organic matter (AOM) (see Table S2, Fig. 5) were conducted, considering size, shape, and preservation state. A quantitative palynofacies approach was employed, counting 250 organic particles per slide following a scheme adapted from Tyson (1995, 1993). The slide would be thoroughly screened to check for anything unexpected that might not have been counted after the 250th particle. Relative counts for all the samples are presented in Table S2. The distribution of palynomorphs and palynofacies counts are summarized in Tables S2 and S3, available in the supplementary material.

Important stratigraphic taxa are illustrated in Figs. 7–10, and selected palynofacies organic particles are shown in Fig. 11 (additional image data, such as samples, files, and coordinates, can be found in Table S4 of the supplementary materials).

5. Results

This study involved the collection of samples from four distinct sections, namely (according to Total-Sonangol, 1987): Quissonde Facies (Mucanzo Formation) - Section VOE-17 and Section VOE-9, Cabo Ledo Formation - Section VOE19, Itombe Formation - Section VOE-13.

In the palynology analysis (Table S2), three main palynology assemblages were identified, with the examined samples

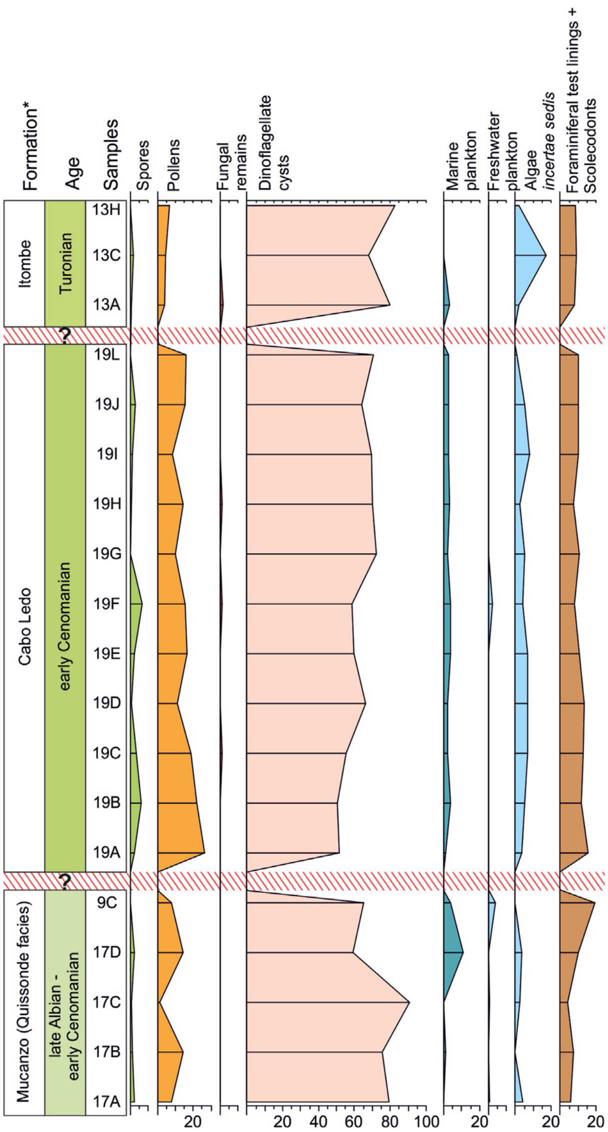

Fig. 4. The palynological summary diagram is subdivided into three assemblages from the late Albian to Turonian age, following biostratigraphic criteria. The boxes shaded in red result from the non-continuity of the sections and the absence of biostratigraphic data in these transitions.

yielding moderately to well-preserved palynomorphs ranging from common to frequent. A total of 7 spore genera and 8 pollen genera (7 pollen species) were identified within the sporomorph subgroup. Additionally, 38 dinoflagellate cysts genera (dinocysts; including 22 species), alongside rare prasinophytes, and acritarchs were identified as part of the marine plankton. Furthermore, very rare occurrences of freshwater plankton and some algae *incertae sedis* (Table S2) were noted. Common to frequent foraminiferal test linings and very rare scolecodonts (Table S2) were also documented.

Regarding the palynofacies (organic facies) analysis (Table S3), the productive samples yielded abundant AOM (ca. 66%). This AOM was mainly composed by abundant irregular-edged, yellow to brown particles in transmitted white light (TWL) and moderate to intense yellow fluorescence in UV-fluorescence light (UVFL; ca. 54%). Additionally, frequent occurrences of sharped subangular particles ranging from dark brown to black color particles (TWL; ca. 11%) were observed, with either absent or weak fluorescence (UVFL). The phytoclast group was also abundant across all samples, mainly due to the frequent presence of the opaque phytoclast subgroup (ca. 16 %), while the other phytoclast subgroups rarely occurred (ca. 2%). Within the palynomorph group (ca. 11%), notable fluctuations in the relative frequencies were observed, largely attributed to the abundance of marine plankton, such as dinoflagellate cysts (ca. 6%, ranging from 0 to 20%).

Below is a description of the main features of the palynological and palynofacies assemblages organized according to the stratigraphic sequence delineated by (according to Total-Sonangol, 1987).

6. Quissonde Facies of Mucanzo Formation – sections VOE-17 and VOE-9

The Quissonde Facies of the Mucanzo Formation yield four productive palynological and palynofacies samples (VOE-17A, VOE-17B, VOE-17C, and VOE-17D; Tables S2 and S3). Spore occurrences were rare (ca. 2%) including *Cicatricosisporites* spp., *Deltoidospora* sp., *Leptolepidites* sp., *Striatella seebergensis*, *Tuberostriletes* sp., and *incertae sedis*. Common pollen occurrences (ca. 10%) included *Araucariacites* sp., *Callialasporites dampieri, Callialasporites trilobatus, Classopollis* spp., *Elaterocolpites castelainii, Elaterocolpites* sp., *Ephedripites* spp., *Gnetaceaepollenites clathratus*, *Gnetaceaepollenites jansonii, Gnetaceaepollenites* spp., *Schizaea certa*, and *Incertae sedis* (Fig. 7).

Palynomorph recovery from section VOE-17 samples was mainly composed of dinocysts (ca. 76%), with notable species including *Apteodinium* sp., *Canningia* sp., *Cribroperidinium* spp., *Coronifera oceanica, Coronifera* sp., *Cyclonephelium* sp., *Circulodinium distinctum*, *Circulodinium* sp., *Dinopterygium cladoides, Exochosphaeridium* spp., *Florentinia laciniata, Florentinia* spp., *Hystrichodinium* sp., *Hystrichosphaeridium* sp., *Nummus monoculatus, Nummus* sp., *Odontochitina costata, Odontochitina* spp., *Oligosphaeridium complex, Palaeohystrichophora infusorioides, Pareodinia* sp., *Subtilisphaera* sp., *Spiniferites* spp., *Tanyosphaeridium* sp., *Xiphophoridium alatum*, *Xenascus ceratioides*, and *incertae sedis* (Figs. 8–10). Other marine plankton were rare (ca. 3%), except for the sample VOE-17D, which presented an exceptional occurrence of acritarchs (*Micrhystridium* sp., ca. 11%). Freshwater plankton was very rare (<1%), alongside other algae *incertae sedis* (2.5%; Fig. 11). Foraminiferal test linings (Fig. 11) were common throughout the interval (ca. 7%), reaching 10% in sample VOE-17D.

The amorphs organic matter group (AOM) dominated the palynofacies assemblage (Fig. 5, Table S3) across all samples (ca. 60%). This group was characterized by irregular-edged, yellow to brown particles under WTL and light-yellow fluorescence (ca. 52%) under UVFL, contrasting with sharped subangular contour particles that ranged from dark brown to black color under WTL and no fluorescence under UVFL; ca. 8%. Opaque phytoclasts accounted for about 10% of the relative abundance, while non-opaque (ca. 5%), membranes (ca. 3%), and fungal remains (ca. 1%) phytoclasts subgroups remained rare. The palynomorph group exhibited frequent relative abundances of marine plankton (dinocysts ca. 13% and acritarchs ca. 1%) and the zoomorph subgroup (foraminiferal test linings ca. 5%).

In contrast, the Quissonde Facies of the Mucanzo Formation sampled in section VOE-9 yielded one poor and poorly preserved palynology sample (VOE-9C, Fig. 4). However, for palynofacies purposes, three samples were considered productive (VOE-9A, VOE-9C, VOE-9D, Fig. 5). Palynomorph recovery from the sample VOE-9C was mainly composed of dinocysts (ca. 65%) including *Exochosphaeridium* spp., *Odontochitina costata*, *Odontochitina operculata*, *Odontochitina* spp., *Oligosphaeridium complex*, and *Subtilisphaera* sp. Foraminiferal test linings were frequent in this sample

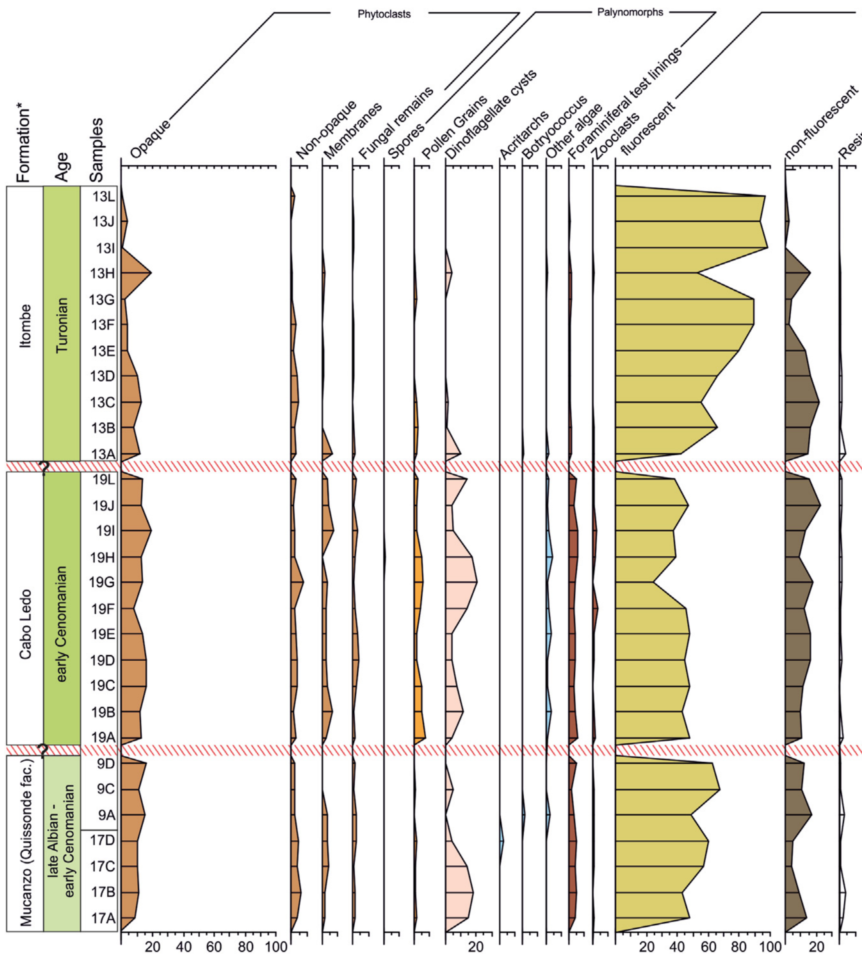

Fig. 5. Palynofacies summary diagram. The boxes shaded in red result from the non-continuity of the sections and the absence of biostratigraphic and paleoenvironment data in these transitions.

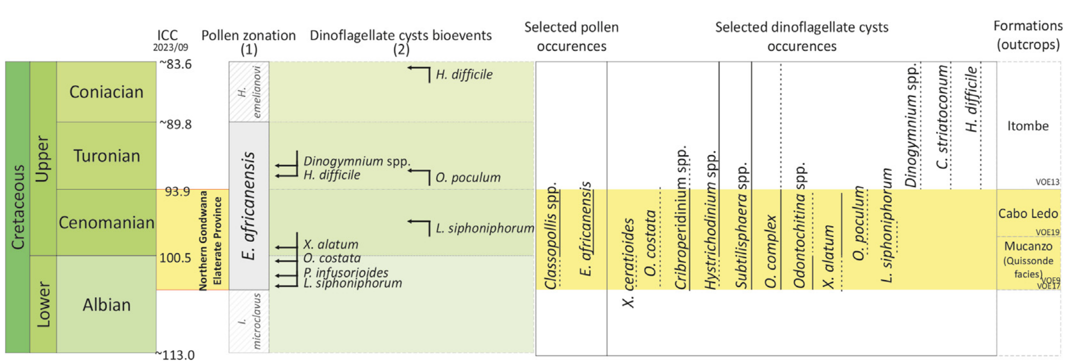

Fig. 6. The dinoflagellate cyst and pollen bioevents scheme established for the Sumbe studied section (Kwanza Basin), based on the combined using pollen and dinoflagellate cyst key taxa and following their first and last occurrences. (1) Pollen zonation following Regali et al. (1974); (2) Dinoflagellate cyst bioevents according to Williams et al. (2004).

(ca. 19%), with no spore recovery, and very rare pollen taxa were documented (8%).

Regarding the palynofacies (Fig. 5, Table S3), the AOM group dominated in all samples (ca. 73%), with a greater abundance of irregular-edged, yellow to brown particles in WTL (ca. 60%) and moderate to intense fluorescence under UVFL, contrasting with sharp-edged subangular particles ranging from dark brown to black color under WTL (ca. 13%) and no fluorescence under UVFL. The relative abundance of opaque phytoclasts was about 14%, while non-opaque (ca. 2%), membranes (ca. 1%), and fungal remains (ca. 2%) phytoclasts subgroups remained rare in this interval. Marine plankton (dinocysts; ca. 2%) and zoomorph subgroups (Foraminiferal test linings; ca. 3%) rarely occurred in the palynomorph group.

7. Cabo Ledo Formation – section VOE19

The Cabo Ledo Formation yielded eleven productive palynological and palynofacies samples (VOE19A, 19B, 19C, 19D, 19E, 19F, 19G, 19H, 19I, 19J, and 19L, Figs. 4 and 5, Tables S2 and S3).

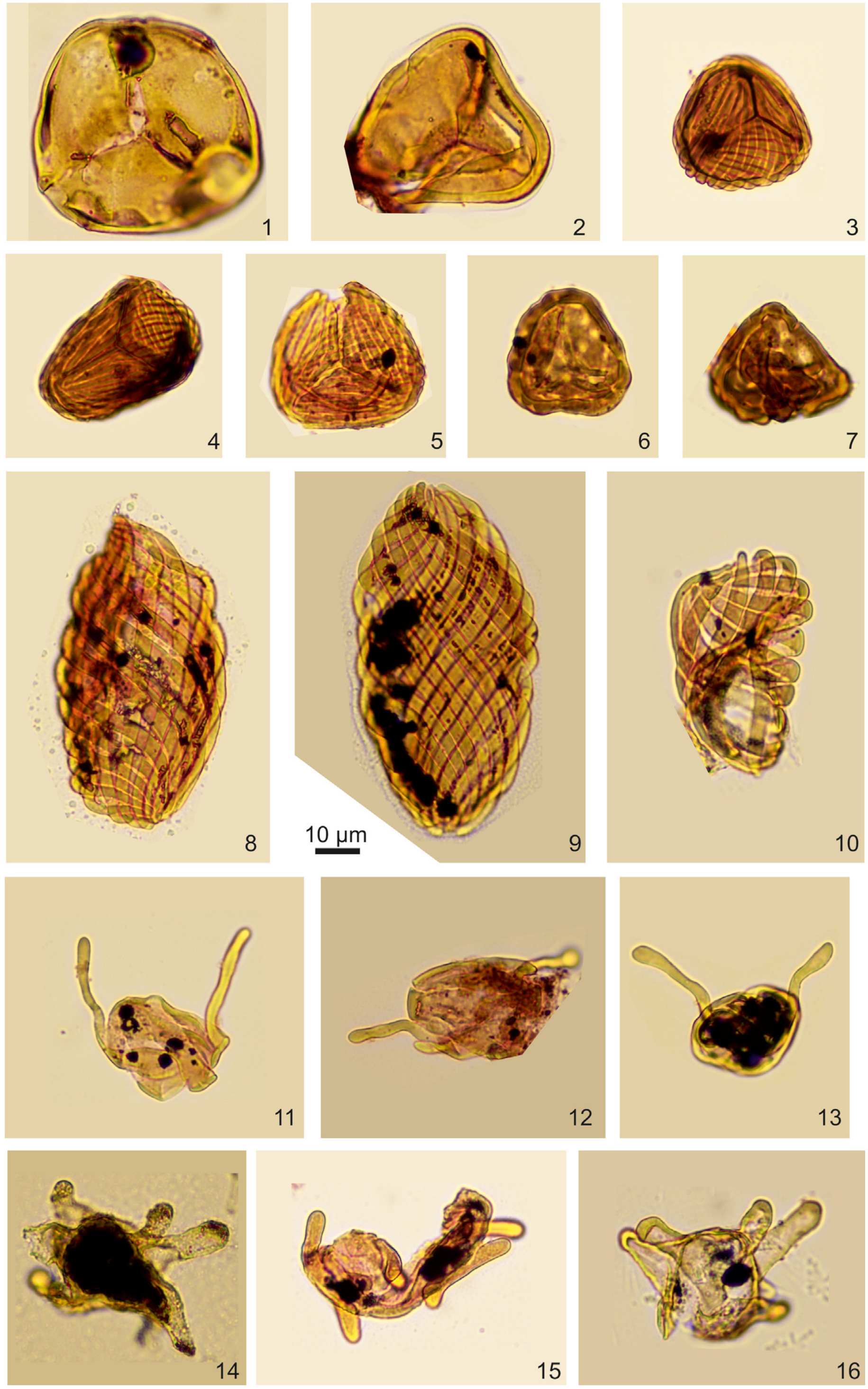

Fig. 7. Selected spore and pollen taxa recovered in the Quissonde and Cabo Ledo formations. See the supplementary materials for additional image data (samples, files, and co-ordinates). 1–2. *Deltoidoispora* sp.; 3–5. *Cicatricosisporites* sp.; 6–7. *Striatella seebergensis* Madler, 1964; 8–9. *Gnetaceaepollenites jansonii* Write (Pocock, 1964) Lima, 1980; 10. *Gnetaceaepollenites* sp.; 11–13. *Elateroplicites africaensis* Hergreen, 1973; 14–16. *Elaterocolpites castelainii* Jardiné and Magloire (1965).

Palynomorph recovery from the marlstones of the VOE19 section was mainly composed of dinocysts (ca. 63%), featuring species such as *Apteodinium* sp., *Canningia* sp., *Cribroperidinium* spp., *Coronifera* sp., *Circulodinium* sp., *Dapsilidinium* sp., *Dinopterygium cladoides*, *Exochosphaeridium* spp., *Florentinia* spp., *Hystrichodinium* sp., *Hystrichosphaeridium* sp., *Heterosphaeridium* sp., *Hystrichodinium pulchrum*, *Hystrichodinium voigtii*, *Hystrichodinium* sp., *Kleithriasphaeridium* sp., *Litosphaeridium siphoniphorum*, *Litosphaeridium* sp., cf. *Muderongia* sp., *Odontochitina costata*, *Odontochitina* spp., *Oligosphaeridium poculum*, *Oligosphaeridium complex*, *Palaeohystrichophora infusorioides*, *Pareodinia* sp., *Pseudoceratium* sp., *Subtilisphaera* sp., *Spiniferites* spp., *Tanyosphaeridium* sp., *Tenua* sp., *Xiphophoridium alatum*, *Walvisia woodii*, and *incertae sedis* (Table S3). Other rare marine plankton (ca. 3%) included prasinophytes algae (*Pterospermella* spp.) and acritarchs (*Micrhystridium* sp.). Freshwater plankton was very rare (<1%), alongside other algae *incertae sedis* (ca.

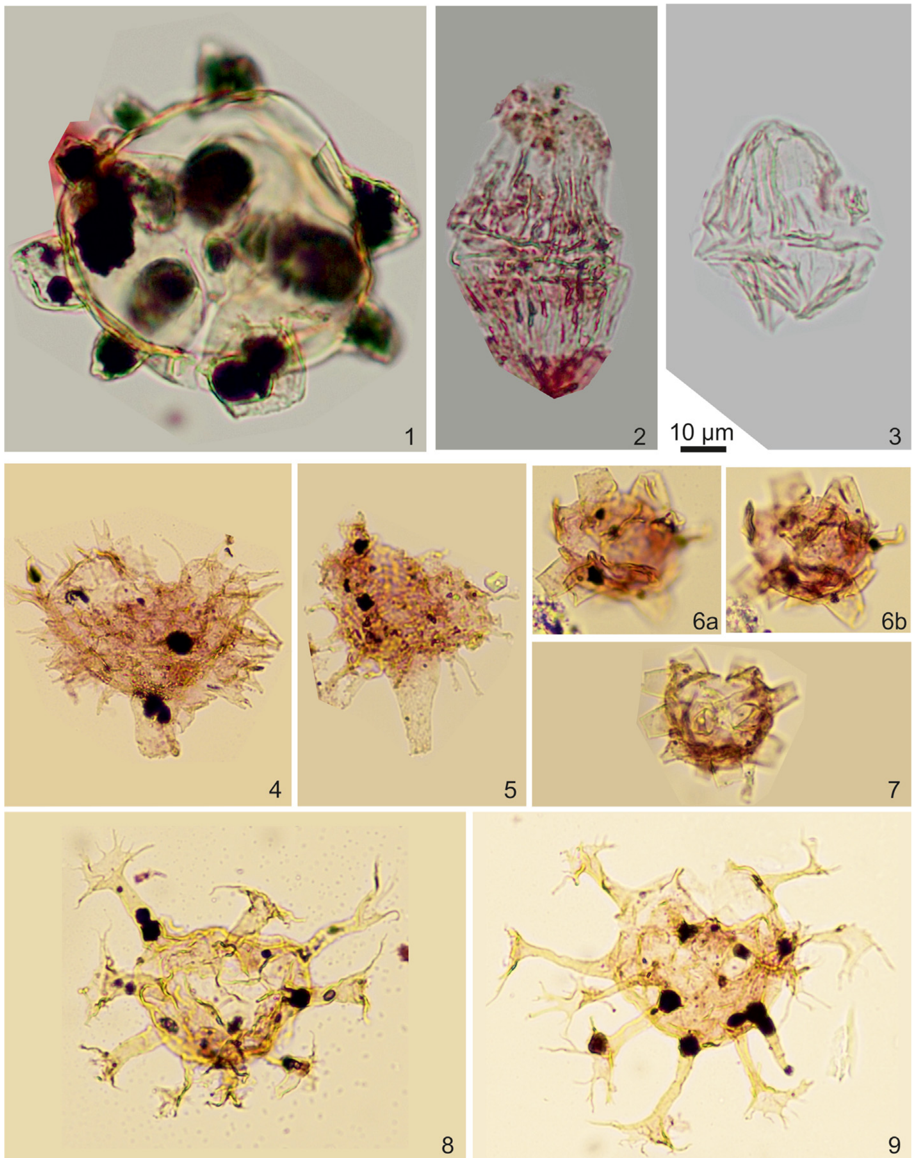

Fig. 8. Selected dinocyst taxa recovered in the Quissonde and Cabo Ledo formations. See the supplementary materials for additional image data (samples, files, and coordinates). 1. *Conosphaeridium striatoconum* (Deflandre and Cookson, 1955) Cookson and Eisenack, 1969; 2–3. *Dinogymnium* sp.; 4. *Florentinia laciniata* Davey and Verdier, 1973; 5. *Coronifera oceanica* Cookson and Eisenack, 1958; 6–7. *Litosphaeridium siphoniphorum* (Cookson and Eisenack, 1958) Davey and Williams, 1966b; 8–9. *Oligosphaeridium complex* (White, 1842) Davey and Williams, 1966b.

5%). Foraminiferal test linings were common to frequent throughout the interval (ca. 11%).

Spore occurrences were rare (ca. 2%), encompassing *Cicatricosisporites* spp., *Deltoidospora* sp., *Striatella seebergensis*, *Tuberostriletes* sp., and *incertae sedis*. Common pollen occurrences (ca. 16%) included *Araucariacites* sp., *Callialasporites dampieri,* rare to abundant *Classopollis* spp., *Elateroplicites africaensis, Ephedripites* spp., *Gnetaceaepollenites jansonii, Gnetaceaepollenites* spp., *Schizaea certa*, and *incertae sedis* (Table S3). Scarce fungal remains were also documented (1%).

Regarding the palynofacies (Fig. 5, Table S3), the AOM group dominated in all samples (ca. 56%), with a greater abundance of irregular-edged, yellow to brown particles under TWL (ca. 42%) with high fluorescence under UVFL, contrasting with sharp-edged subangular particles ranging from dark brown to black color under TWL (ca. 14%) with no fluorescence under UVFL. The relative abundance of opaque phytoclasts was about 14%, while non-opaque (ca. 3%), membranes (ca. 4%), and fungal remains (ca. 2%) phytoclasts subgroups remained rare in this interval. In the palynomorph group, frequent relative abundances of marine plankton (dinocysts, ca. 10%), pollen (ca. 3%), and the zoomorph subgroups (including foraminiferal test linings, ca. 4%) were notable.

8. Itombe Formation – section VOE-13

Palynomorph recovery from the samples of section VOE-13 was mainly composed of dinocysts (ca. 77%), particularly with *Alisogymnium deflandrei*, *Alisogymnium* sp., *Canningia* sp., *Cerbia* sp., *Cribroperidinium* spp., *Conosphaeridium striatoconum*, *Coronifera* sp., *Cyclonephelium* sp., *Circulodinium* sp., *Dinogymnium acuminatum, Dinogymnium* sp., *Exochosphaeridium* spp., *Florentinia* cf. *clavigera*, *Florentinia mantellii*, *Florentinia* spp., *Hystrichodinium* sp., *Hystrichosphaeridium* sp., *Heterosphaeridium difficile, Heterosphaeridium* sp., *Hystrichodinium pulchrum,*

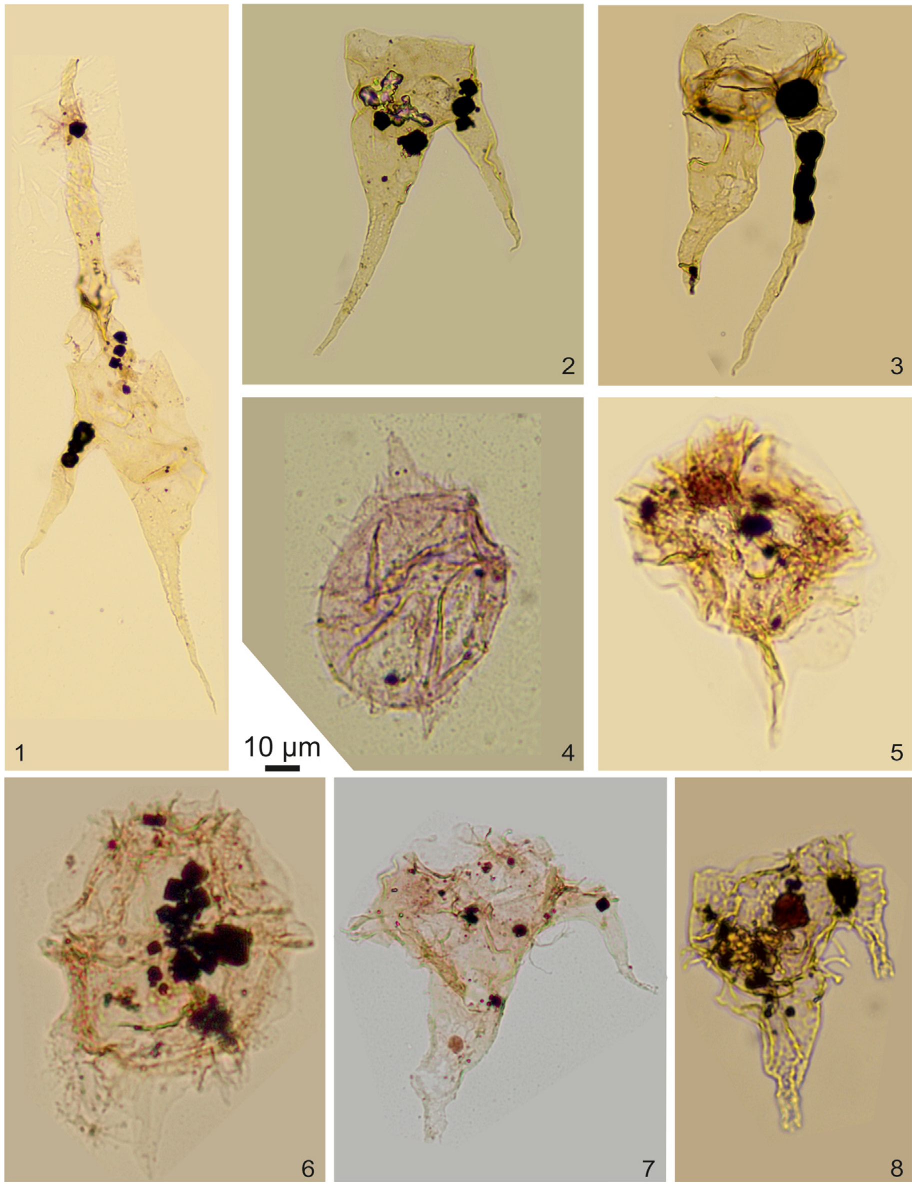

Fig. 9. Selected dinocyst taxa recovered in the Quissonde and Cabo Ledo formations. See the supplementary materials for additional image data (samples, files, and coordinates). 1–3. *Odontochitina costata* (Alberti, 1961) Clarke and Verdier, 1967. 4. *Palaeohystrichophora infusorioides* Deflandre, 1935; 5–6. *Xiphophoridium alatum* (Cookson and Eisenack, 1962b) Sarjeant, 1966b; 7–8. *Xenascus ceratioides* (Deflandre, 1937b) Lentin and Williams, 1973.

Hystrichodinium voigtii, *Hystrichodinium* sp., *Impagidinium* sp., *Kallosphaeridium* sp., *Systematophora* sp., *Odontochitina costata*, *Odontochitina* spp., *Oligosphaeridium complex*, *Palaeohystrichophora infusorioides*, *Phelodinium* sp., *Senoniasphaera* sp., *Subtilisphaera* sp., *Spiniferites* spp., *Tenua* sp., *Walvisia woodii*, and *incertae sedis* (Table S2).

There was no record of freshwater plankton, while other marine plankton (ca. 1%) including very rare prasinophytes algae (*Pterospermella* spp.), was documented. Foraminiferal test linings were common to frequent throughout the interval (ca. 8%).

Spore occurrences were rare (<1%), including *Cicatricosisporites* spp., and *Deltoidospora* sp. The rare pollen occurrences (ca. 5%) were assigned to *Ephedripites* spp., *Gnetaceaepollenites* spp., *Schizaea certa*, and *incertae sedis*. Scarce fungal remains were also documented (<1%).

Regarding the palynofacies (Fig. 5, Table S2), the AOM group was dominant in all samples (ca. 85%), with a greater abundance of irregular-edged, yellow to brown particles (TWL, ca. 75%) with high fluorescence under UVFL, contrasting with sharp-edged subangular particles ranging from dark brown to black color under TWL (ca. 10%) with no fluorescence under UVFL. The relative abundance of opaque phytoclasts was about 7%, while non-opaque (ca. 2%), membranes (ca. 1%), and fungal remains (<1%) phytoclasts subgroups remained rare in this interval. All palynomorph subgroups were rare (ca. 4%), with rare marine plankton occurrences (dinocysts ca. 2%), particularly noted in sample VOE-13A.

9. Discussion

9.1. Age

The palynomorph assemblages retrieved from the studied sections, including VOE-17, VOE-9, VOE-19, and VOE-13, provide

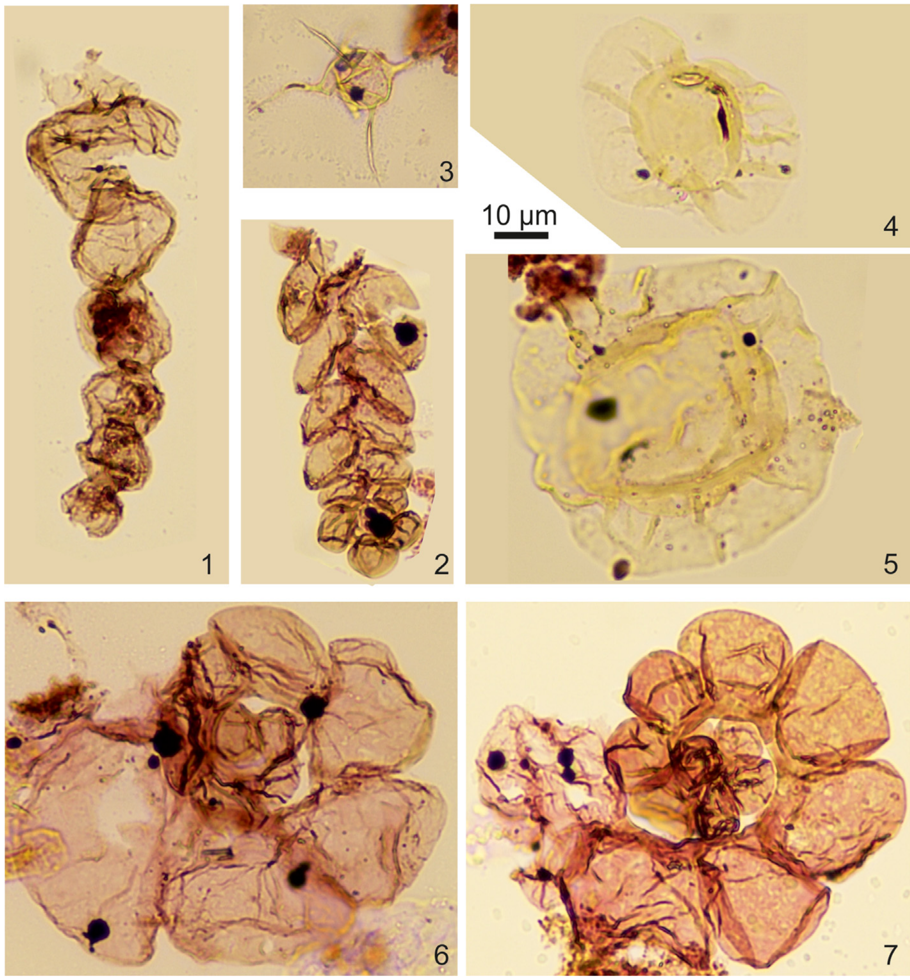

Fig. 10. Selected acritarchs, algae, and Foraminiferal test linings taxa recovered in the Cabo Ledo Formation. See the supplementary materials for additional image data (samples, files, and coordinates). 1–2, 6–7. Foraminiferal test linings; 3. *Micrhystridium* sp.; 4–5. *Pterospermella* sp.

valuable insights into the late Albian–Turonian interval age (Figs. 4 and 6).

In the Quissonde Facies of Mucanzo Formation samples (VOE-17 and VOE-9), dinocysts such as *Odontochitina costata, Palaeohystrichophora infusorioides,* and *Xiphophoridium alatum* are prominent. Additionally, during this interval, an acme of *Oligosphaeridium complex* (ca. 25%) is documented (Figs. 4 and 6). These species are indicative of a late Albian to lower Cenomanian age, aligning with previous findings, notably the dating of pelagic foraminifera by Meijer (1989) and Morais et al. (1990) within the Quissonde Facies of Mucanzo and Cabo Ledo formations.

Thus, for the Quissonde Facies of Mucanzo Formation samples studied in this research, an upper Albian–lower Cenomanian age is suggested in light of these occurrences.

In the Cabo Ledo Formation samples (VOE-19), key species such as *Odontochitina costata* (NML 99.65 Ma Williams et al., 2004) and *Palaeohystrichophora infusorioides* (NML 99.85 Ma Williams et al., 2004) are frequently observed. These cysts were previously recorded as first occurring during the late Albian in Northern Hemisphere mid-latitudes (*e.g.,* Williams et al., 2004). In the same way, the first occurrence of *Xiphophoridium alatum* suggests a younger age in Northern Hemisphere high latitudes since it first occurred in the early Cenomanian (NHL 98.02 Ma). Also, the co-occurrence of *Litosphaeridium siphoniphorum* cyst further supports a late Albian to Turonian age, with the presence of *Oligosphaeridium poculum* suggesting an age no younger than early Turonian. The *Litosphaeridium siphoniphorum* cyst is commonly used as a key species since it first occurs during the late Albian (NML 101.6 Ma Williams et al., 2004) and last occurs during the middle Cenomanian age (SML 95? Ma Williams et al., 2004). At the same time, in the Northern Hemisphere, his last occurrence is documented later in the late Cenomanian age (NML 93.81 Ma Williams et al., 2004). Still, in this assemblage, the rare occurrence of *Oligosphaeridium poculum* also established an age no younger than early Turonian (LO NML 91.88 Ma).

Additionally, the occurrence of key species *Elaterocolpites castelainii* pollen reinforces an Albian–Cenomanian age considering it was highly recovered in the middle Albian - Turonian in Brazil (Herngreen, 1973, 1975; Regali et al., 1974; Arai and Botelho Neto, 1996; Dino et al., 1999), late Albian–lower Cenomanian in Dongola region in northern Sudan (Schrank, 1990), Gabon and Senegal (Jardiné, 1967), Colombia (Herngreen and Duenas Jimenez, 1990), Egypt (Zobaa et al., 2013), upper Albian–upper Cenomanian in Senegal (Jardiné and Magloire, 1965), Albian in Gabon (Boltenhagen, 1965), Albian in Libya (Thusu and Van Der Eem, 1985), upper Albian - middle Cenomanian in Nigeria (Abubakar et al., 2006, 2011). The presence of elater-bearing pollen, such as *Elaterocolpites castelainii* and *Elateroplicites africaensis,* in samples VOE-17 and VOE19, corresponds to the diversity and frequency climax levels observed during the late Albian–Cenomanian (*e.g.,* Dino et al., 1999). Following this climax, there's a decrease in temperature towards the end of the Cenomanian, leading to the disappearance of elaterate pollen from the stratigraphic record (Dino et al., 1999). This is also

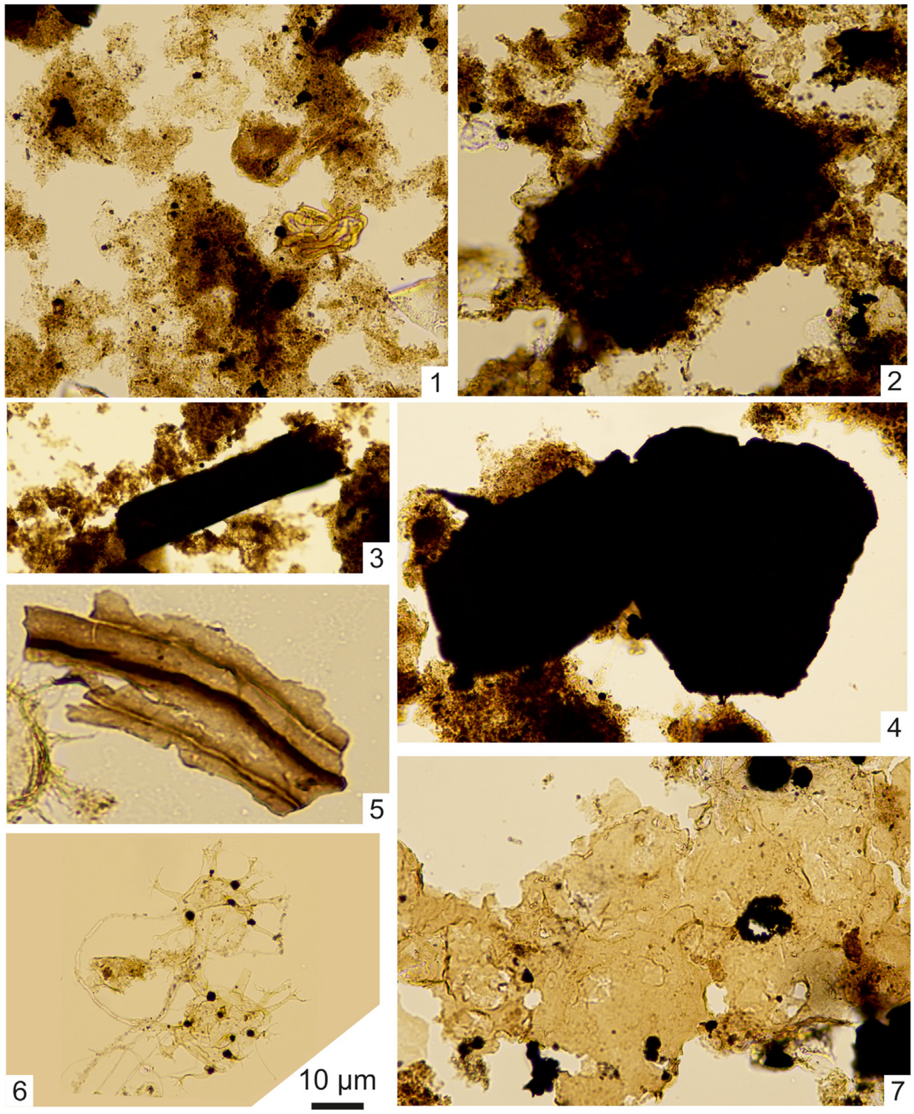

Fig. 11. Illustration of the palynofacies groups documented in this research. 1. Amorphous organic matter and one pollen grain. 2. Amorphous organic matter from phytoclast origin; 3–4. Opaque phytoclasts; 5. Non-opaque phytoclasts; 6. Dinoflagellate cysts; 7. Membrane.

observed in other mid-Cretaceous units from West Africa, such as Côte D'Ivoire-Ghana (Kaska, 1989; Masure et al., 1998; Atta-Peters, 2013). Thus, altogether, the palynomorph assemblages from the Cabo Ledo Formation indicate a Cenomanian age.

In the Itombe Formation samples (VOE-13), the rare occurrence of the *Conosphaeridium striatoconum*, as well as rare *Heterosphaeridium difficile, Dinogymnium acuminatum,* and *Dinogymnium* sp. cysts (Figs. 4 and 6) suggests a Turonian age. *Dinogymnium* spp. (Schiøler et al., 2012 personal communication; NML 91.69 Ma Williams et al., 2004) cyst first occurred during the early Turonian, in the same way as the *Heterosphaeridium difficile* (NML 92.15 Ma) cyst. Despite the occurrence of *Dinogymnium* spp. lasted until the end of the Cretaceous, the *Heterosphaeridium difficile* was found only until the end of the Coniacian (NML 86.78 Ma Williams et al., 2004). In the same way, the *Conosphaeridium striatoconum* dinocyst has been documented exclusively from the Southern Hemisphere, particularly in the Coniacian age, with the last occurrence documented at the top of the Coniacian (*e.g.*, Smith et al., 1994; Williams et al., 2004; Schiøler et al., 2012).

Furthermore, within the Itombe Formation, Late Cretaceous echinoderm taxa have been identified (Haughton, 1924; Kier and Lawson, 1978; Néraudeau and Mathey, 2000). In the Angola Continental Margin, significant biostratigraphic studies of the Cretaceous have also been conducted, focusing on foraminifers and nannoplankton by Bruno et al. (2020) and Magniez-Jannin and Muller (1987). These studies suggest an Albian–Cenomanian age for the studied section, although lithostratigraphic correlation remains unclear. Regarding these findings, a Turonian age is suggested for the Itombe Formation samples studied in this research (Fig. 6).

Overall, the palynomorph data corroborate the ages suggested by other fossil groups and provide additional evidence for the late Albian to Turonian interval age in the studied sections.

10. Paleoenvironments, paleoclimates and paleogeography

The palynofacies and paleoenvironment characterization of the VOE-17, VOE-9, VOE19, and VOE-13 sections provide insights into the depositional conditions, paleoclimate, and paleogeography during the late Albian to Turonian interval.

Firstly, all samples from these lithostratigraphic units exhibit high contents of AOM (Fig. 5, Table S3), suggesting distal depositional settings under dysoxic-anoxic conditions (Tyson, 1993, 1995). This indicates reducing conditions favoring the preservation of AOM, likely due to a lack of terrestrial organic matter input (Tyson, 1993). Moreover, a significant increase in AOM at the top of the sequence (Itombe Formation, VOE-13 samples, Fig. 5, Table S3) suggests variations in the water column, possibly indicating a thicker water column and more distal setting in the younger sediments (Tyson and Follows, 2000; Zobaa et al., 2011a, 2011b; Mueller et al., 2014). This intense burial of organic matter could be attributed to heightened primary productivity or improved preservation scenarios (Schlanger and Jenkyns, 1976a; Schlanger et al., 1987), particularly evident at the Cenomanian/Turonian boundary. However, the trigger mechanism remains unclear, and more organic geochemical analyses are needed.

Furthermore, the palynomorph group, particularly dinoflagellate cysts, provides environmental details. Common to abundant *Subtilisphaera* cysts (ranging from 9 to 39%, ca. 15%, Table S2) suggest an inner-neritic environment, known as “*Subtilisphaera* Ecozone” (*e.g.,* Arai et al., 1994, 2000). Additionally, the restricted occurrence of *Xenascus ceratioides* in the VOE-17B sample (Table S2), as well as scarce and sparse occurrences of *Xenascus* sp., are usually associated with restricted shallow marine (Tocher and Jarvis, 1987; Skupien and Mohamed, 2008)) and low to varying salinity settings (Lister and Batten, 1988; Wilpshaar and Leereveld, 1994).

Paleoclimate indicators, such as elater-bearing pollen species (*e.g., E. castelainii* and *E. africanensis*) and other Gnetalean pollen (*e.g., G. clathratus, G. jansonii, Gnetaceaepollenites* spp., *Ephedripites* spp.) suggests a subtropical to tropical climate (*e.g.*, (Herngreen and Duenas Jimenez, 1990; Herngreen et al., 1996; Schrank, 2001; Kolonic et al., 2005; Wang et al., 2011; Hu et al., 2012; Strganac et al., 2014; Bruno et al., 2022), consistent with the Northern Gondwana Elaterate Province (Brenner, 1976; Srivastava, 1981). This reflects the rapid diversification of flora (*e.g.,* Dino et al., 1999; Atta-Peters, 2013) in response to mid-Cretaceous climatic alterations, and probably related to the mid-Cretaceous Oceanic Anoxic Event (OAE2). This phenomenon is linked to the rapid diversification of flora (*e.g.*, Dino et al., 1999; Atta-Peters, 2013) in response to mid-Cretaceous climatic changes, likely associated with the mid-Cretaceous Oceanic Anoxic Event (OAE2). Also known as the Cenomanian-Turonian event, around 93 million years ago (Schlanger and Jenkyns, 1976b), this event is marked by severe disruptions in the global carbon cycle, affecting ocean basins worldwide and significantly influencing both fauna and flora (Gangl et al., 2019). These impacts are particularly evident in Brazilian sedimentary successions, which correspond to West African basins such as the Kwanza Basin (Arai, 1988; Mello et al., 1989; Koutsoukos et al., 1990, 1991; Rodrigues, 2005; Tedeschi et al., 2017; Valle et al., 2019). Additionally, these authors have highlighted the presence of black shales and marls containing marine organic matter, frequently found interlayered with organic-poor claystones and bioturbated limestones in the South Atlantic Ocean. This suggests that during OAE2, anoxic conditions experienced periodic fluctuations, likely due to cyclic changes in the mid-water oxygen minimum zone depth, influenced by increased rates of seafloor spreading, elevated sea levels, and reduced water circulation (Jacquin and de Graciansky, 1988; Koutsoukos et al., 1991; Valle et al., 2019). Consequently, the samples analyzed in the Sumbe region exhibit palynological indications of OAE2, such as intervals of oceanic anoxia, reflected in the palynological record by increased terrestrial pollen and spores, indicating terrestrial organic matter input into the ocean during periods of marine plankton reduction.

The continental breakup of the Gondwana brought significant changes in global paleogeographic configurations, notably forming and expanding the South Atlantic Ocean (*e.g.,* Atta-Peters, 2013; Granot and Dyment, 2015). Paleogeographic evidence gathered from palynology assemblages recovered in the Quissonde Facies (Mucanzo Formation) and Cabo Ledo Formation, spanning the late Albian to Cenomanian age, can corroborate global models, particularly within the Kwanza Basin. The presence of elater-bearing pollen during this period holds significant importance to understand the paleoenvironment, paleoclimatic and paleogeographic conditions, directly correlating with the Elaterates Province (according to Herngreen et al., 1996), recognized in several paleoequatorial sites across South America (*e.g.,* Brazil, Dino et al., 1999; Herngreen, 1973, 1975; Colombia, Herngreen and Duenas Jimenez, 1990) and African countries (*e.g.,* Algeria, Angola, Congo, Egypt, Zobaa et al., 2013; Gabon and Senegal, Boltenhagen, 1965; Jardiné, 1967; Jardiné and Magloire, 1965; Sudan, Schrank, 1990; Nigeria, Abubakar et al., 2006, 2011; Libya, Thusu and Van Der Eem, 1985). The diversification and abundance of elater-bearing plants, typical found in arid regions under warm climates, may be linked to climatic changes associated with the breakup and widening of the northern parts of the South Atlantic Ocean (during the latest Aptian to early Albian and ending during the late Albian–Cenomanian; Dino et al., 1999; Abubakar et al., 2006).

Dinocyst assemblages recorded in this study, indicating a predominant Tethyan influence marked by the occurrence of a recognized Tethyan affinity species, such as *Subtilisphaera* spp. (Arai, 2014; Arai et al., 2000), *Spiniferites* sp. (Carvalho et al., 2016), *Florentinia* sp. (Skupien and Vasicek, 2002), and *Xenascus ceratioides* (Masure et al., 2013), further support the breakup. Additionally, the presence of cosmopolitan taxa like *Xiphophoridium alatum*, with high latitude affinities (Williams et al., 2004; Masure et al., 2013), becomes more pronounced and consistent from the Cenomanian age (Cabo Ledo Formation), likely related to Atlantic Ocean water flows from north to south following the onset of continental breakup.

Thus, the subtropical to the tropical affinity of pollen assemblages, coupled with dinoflagellates showing Tethyan affinity, suggests an open connection between the Central Atlantic and South Atlantic oceans since the mid-Cretaceous, extending at least to the Kwanza Basin.

11. Conclusions

The palynological study of the Quissonde Facies of the Mucanzo Formation and Cabo Ledo and Itombe formations yields the following conclusions.

- The Quissonde Facies (Mucanzo Formation) spans from the upper Albian to lower Cenomanian, based on the co-occurrence of *Odontochitina costata, Palaeohystrichophora infusorioides,* and *Xiphophoridium alatum* dinocysts. The Cabo Ledo Formation age is dated from the Cenomanian, based on the occurrence of *Litosphaeridium siphoniphorum* cyst and the *Elateroplicites africaensis* pollen, together with *Odontochitina costata, Palaeohystrichophora infusorioides,* and *Xiphophoridium alatum.* The Itombe Formation age is dated from the Turonian based on the co-occurrence of *Conosphaeridium striatoconum*, *Heterosphaeridium difficile, Dinogymnium acuminatum,* and *Dinogymnium* sp. cysts. These palynostratigraphy ages aligns with earlier biostratigraphic studies conducted on different fossil groups.
- Samples from Quissonde Facies of the Mucanzo Formation, Cabo Ledo, and Itombe formations predominantly exhibit fluorescent AOM, indicating inner marine deposition mostly under dysoxic-anoxic depositional conditions. Fluctuations in the water column are also evident.

- The subtropical to tropical flora observed in the Quissonde Facies of the Mucanzo Formation and Cabo Ledo Formation (upper Albian to Cenomanian) reflects arid to semi-arid palaeoclimatic conditions, probably linked to climatic changes associated with continental breakup and the spreading of the northern South Atlantic Ocean.
- Palynology and palynofacies assemblages of the Mucanzo Formation and Cabo Ledo Formation (upper Albian to Cenomanian) potentially reflect a mid-Cretaceous Oceanic Anoxic Event. This is indicated by an increase in terrestrial pollen and spores, suggesting a rise in terrestrial organic matter input into the ocean during periods of reduced marine plankton.
- Lastly, the presence of cosmopolitan taxa with a higher latitude affinity suggests a predominant Tethyan influence, likely responding to mid-Cretaceous paleogeographic changes. This implies an open connection between the Central Atlantic and South Atlantic oceans, extending at least to the Kwanza Basin.

CRediT authorship contribution statement

Cristina Rodrigues: Writing – review & editing, Validation, Supervision, Formal analysis, Conceptualization. **Márcia Mendes:** Writing – review & editing, Writing – original draft, Visualization, Validation, Supervision, Software, Resources, Project administration, Methodology, Investigation, Formal analysis, Data curation, Conceptualization. **Zélia Pereira:** Writing – review & editing, Validation, Supervision, Investigation, Formal analysis, Conceptualization. **Pedro Claude Nsungani:** Writing – review & editing, Resources, Project administration, Conceptualization. **Paulo Fernandes:** Validation, Supervision, Investigation, Conceptualization. **Luís Vítor Duarte:** Validation, Supervision, Investigation. **Belarmino Chitangueleca:** Validation, Resources, Project administration, Funding acquisition, Conceptualization. **Lúmen Sebastião:** Validation, Resources. **Benedito Aida:** Validation, Investigation. **Davide Degli Esposti:** Validation, Investigation. **Domingos Freitas:** Validation.

Declaration of competing interest

The authors declare that they have no known competing financial interests or personal relationships that could have appeared to influence the work reported in this paper.

Data availability

No data were used for the research described in the article.

Acknowledgments

The data provided in this paper forms part of an interdisciplinary research project called “Quicombo/Sumbe Field Trip.” Various analytical techniques, including palynostratigraphy, sedimentology, organic maturation, and organic geochemistry, were employed to investigate the studied formations. This project was possible through collaborative efforts between Victory Oil & Energy, ANPG (Agência Nacional de Petróleo, Gás e Biocombustíveis), and PGS. The authors express their gratitude to Victory Oil & Energy Company for providing access to samples and complementary information.

Special thanks are extended to the technicians Irene Sousa and Margarida Valente from LNEG for their invaluable assistance with laboratory support and sample preparation. Appreciation is also extended to the Editor-in-Chief Maria Rose Petrizzo, and two anonymous reviewers for their insightful comments and suggestions, which significantly contributed to the enhancement of the manuscript's quality. Their input is sincerely acknowledged.

References

Abubakar, M.B., Obaje, N.G., Luterbacher, H.P., Dike, E.F.C., Ashraf, A.R., 2006. A report on the occurrence of Albian-Cenomanian elater-bearing pollen in Nasara-1 well, Upper Benue Trough, Nigeria: biostratigraphic and palaeoclimatological implications. Journal of African Earth Sciences 45, 347–354. https://doi.org/10.1016/j.jafrearsci.2006.03.008.

Abubakar, M.B., Luterbacher, H.P., Ashraf, A.R., Ziedner, R., Maigari, A.S., 2011. Late Cretaceous palynostratigraphy in the Gongola Basin (Upper Benue Trough, Nigeria). Journal of African Earth Sciences 60, 19–27. https://doi.org/10.1016/j.jafrearsci.2011.01.007.

Arai, M., 1988. Geochemical reconnaissance of the Mid-Cretaceous anoxic event in the Santos Basin, Brazil. Revista Brasileira de Geociencias 18, 273–282.

Arai, M., 2014. Aptian/Albian (early cretaceous) paleogeography of the south Atlantic: a paleontological perspective. Brazilian Journal of Geology. https://doi.org/10.5327/Z2317-4889201400020012.

Arai, M., Botelho Neto, J., 1996. Biostratigraphy of the marine Cretaceous of the southern and southeastern Brazilian marginal basins, based on dinoflagellates. IGCP Project381: South Atlantic Mesozoic Correlations 408–410.

Arai, M., Lana, C.C., Pedrão, E., 1994. Ecozona Subtilisphaera spp.: Registro eocretaceo de um importante episodio ecologico do Oceano Atlantico primitivo. Acta Geologica Leopoldensia 39, 521–538.

Arai, M., Botelho Neto, J., Lana, C.C., Pedrão, E., 2000. Cretaceous dinoflagellate provincialism in Brazilian marginal basins. Cretaceous Research 21, 351–366. https://doi.org/10.1006/cres.2000.0211.

Atta-Peters, D., 2013. Occurrences of elaterate pollen from the Lower Cretaceous of Ghana: implications for biostratigraphy and palaeoclimatology. International Letters of Natural Sciences 4, 54–66.

Barron, E.J., Thompson, S.L., Schneider, S.H., 1981. An Ice-Free Cretaceous? Results from climate model simulations. Science 212 (1979), 501–508. https://doi.org/10.1126/science.212.4494.501.

Bodin, S., Meissner, P., Janssen, N.M.M., Steuber, T., Mutterlose, J., 2015. Large igneous provinces and organic carbon burial: controls on global temperature and continental weathering during the Early Cretaceous. Global Planetary Changes 133, 238–253. https://doi.org/10.1016/j.gloplacha.2015.09.001.

Boltenhagen, E., 1965. Introduction à la palynology stratigraphique du bassin sédimentaire de l'Afrique équatoriale. Mémoires du Bureau de recherches géologiques et minières 32, 305–326.

Brenner, G.J., 1976. Middle Cretaceous floral provinces and early migration of angiosperms. In: Beck, C.B. (Ed.), Origin and Early Evolution of Angiosperms. Columbia University Press, pp. 1–10.

Brognon, G.P., Verrier, G.R., 1966. Oil and Geology in Cuanza Basin of Angola, vol. 50. American Association of Petroleum Geologists, pp. 108–153.

Brownfield, M., Charpentier, R., 2006. Geology and total petroleum systems of the West Central Coastal province, 2207-B. U.S Geological Survey Bulletin, West Africa.

Bruno, M.D.R., Fauth, G., Watkins, D.K., Savian, J.F., 2020. Albian–Cenomanian calcareous nannofossils from DSDP Site 364 (Kwanza Basin, Angola): biostratigraphic and paleoceanographic implications for the South Atlantic. Cretaceous Research 109, 104377. https://doi.org/10.1016/j.cretres.2020.104377.

Bruno, M.D.R., Fauth, G., Watkins, D.K., Caramez, M.G. da S., Nauter-Alves, A., Savian, J.F., 2022. Paleoceanographic evolution in the South Atlantic Ocean (Kwanza Basin, Angola) during its post-salt foundering. Marine and Petroleum Geology 144, 105852. https://doi.org/10.1016/j.marpetgeo.2022.105852.

Buta-Neto, A., Tavares, T.S., Quesne, D., Guiraud, M., Meister, C., David, B., Duarte-Morais, M.L., 2006. Synthèse préliminaire des travaux menés sur le bassin de Benguela (Sud d'Angola): implications sédimentologiques et structurales. Africa Geoscience Review 13, 239–250.

Carvalho, G.S. de, 1961. Geologia do Deserto de Moçâmedes: (Angola): Uma contribuição para o Conhecimento dos Problemas da Orla Sedimentar de Moçâmedes. Memórias da Junta de Investigações do Ultramar 1–227.

Carvalho, M.D.A., Bengtson, P., Lana, C.C., 2016. Late Aptian (Cretaceous) paleoceanography of the South Atlantic Ocean inferred from dinocyst communities of the Sergipe Basin, Brazil. Paleoceanography 31, 2–26. https://doi.org/10.1002/2014PA002772.

Chumakov, N.M., Zharkov, M.A., German, A.B., Doludenko, M.P., Kalandadze, N.N., Lebedev Ye, L., Ponomarenko, A.G., Rautian, A.S., 1995. Klimaticheskiye poyasa v seredine melovogo perioda. Stratigrafiya. Geologicheskaya Korrelyatsiya 3, 42–63.

Clarke, L.J., Jenkyns, H.C., 1999. New oxygen isotope evidence for long-term Cretaceous climatic change in the Southern Hemisphere. Geology 27, 699. https://doi.org/10.1130/0091-7613(1999)027<0699:NOIEFL>2.3.CO;2.

Cooper, M.R., 2003a. Stratigraphy and paleontology of the Upper Cretaceous (Santonian) Baba formation at São Nicolau, Angola. Annals of the South African Museum 110, 147–170.

Cooper, M.R., 2003b. Upper Cretaceous Ammonites (Turonian-Coniacian) from São Nicolau. Annals of the South African Museum 110, 89–146.

Dino, R., Pocknall, D.T., Dettmann, M.E., 1999. Morphology and ultrastructure of elater-bearing pollen from the Albian to Cenomanian of Brazil and Ecuador:

implications for botanical affinity. Review of Palaeobotany and Palynology 105, 201–235. https://doi.org/10.1016/S0034-6667(98)00076-1.
Fensome, R.A., Taylor, F.J.R., Norris, G., Sarjeant, W.A.S., Wharton, D.I., Williams, G.L., 1993. A classification of living and fossil dinoflagellates. Micropaleontology 39, 295–296.
Fensome, R.A., MacRae, R.A., Williams, G.L., 2008. DINOFLAJ2 [WWW Document]. American Association of Stratigraphic Palynologists, Data Series, Version 1.
Föllmi, K.B., 2012. Early Cretaceous life, climate and anoxia. Cretaceous Research 35, 230–257. https://doi.org/10.1016/j.cretres.2011.12.005.
Friedrich, O., Norris, R.D., Erbacher, J., 2012. Evolution of middle to Late Cretaceous oceans – A 55 m.y. record of Earth's temperature and carbon cycle. Geology 40, 107–110. https://doi.org/10.1130/G32701.1.
Gangl, S.K., Moy, C.M., Stirling, C.H., Jenkyns, H.C., Crampton, J.S., Clarkson, M.O., Ohneiser, C., Porcelli, D., 2019. High-resolution records of Oceanic Anoxic Event 2: insights into the timing, duration and extent of environmental perturbations from the palaeo-South Pacific Ocean. Earth and Planetary Science Letters 518, 172–182. https://doi.org/10.1016/j.epsl.2019.04.028.
Granot, R., Dyment, J., 2015. The Cretaceous opening of the South Atlantic Ocean. Earth and Planetary Science Letters 414, 156–163. https://doi.org/10.1016/j.epsl.2015.01.015.
Guiraud, M., Buta-Neto, A., Quesne, D., 2010. Segmentation and differential post-rift uplift at the Angola margin as recorded by the transform-rifted Benguela and oblique-to-orthogonal-rifted Kwanza basins. Marine and Petroleum Geology 27, 1040–1068. https://doi.org/10.1016/j.marpetgeo.2010.01.017.
Haughton, S.H., 1924. Notes sur quelques fossiles crétacés de l'Angola (Céphalopodes et Échinides). Comunicacoes dos Servicos Geologicos de Portugal 15, 79–106.
Herngreen, G.F.W., 1973. Palynology of the Albian – Cenomanian strata of borehole 1 – QS – 1 – MA. State of Maranhao, Brazil. Pollen et Spores 15, 515–555.
Herngreen, G.F.W., 1975. Palynology of Middle and Upper Cretaceous strata in Brazil. Mededelingen Rijks Geologische Dienst 26, 39–91.
Herngreen, G.F.W., Duenas Jimenez, H., 1990. Dating of the Cretaceous Une Formation, Colombia and the relationship with the Albian-Cenomanian African-South American microfloral province. Review of Palaeobotany and Palynology 66, 345–359. https://doi.org/10.1016/0034-6667(90)90046-L.
Herngreen, G.F.W., Kedves, M., Rovnina, L.V., Smirnova, S.B., 1996. Cretaceous palynofloral provinces: a review. In: Jansonius, J., McGregor, D.C. (Eds.), Palynology: Principles and Applications. American Association of Stratigraphic Palynologists Foundation, pp. 1157–1188.
Hu, X., Wagreich, M., Yilmaz, I.O., 2012. Marine rapid environmental/climatic change in the Cretaceous greenhouse world. Cretaceous Research 38, 1–6. https://doi.org/10.1016/j.cretres.2012.04.012.
Jacquin, T., de Graciansky, P.Ch, 1988. Cyclic fluctuations of anoxia during Cretaceous time in the South Atlantic Ocean. Marine and Petroleum Geology 5, 359–369. https://doi.org/10.1016/0264-8172(88)90029-3.
Jardiné, S., 1967. Spores á expansion en forme d'élatéres du crétacé moyen d'afrique occidentale. Review of Palaeobotany and Palynology 1, 235–258. https://doi.org/10.1016/0034-6667(67)90126-1.
Jardiné, S., Magloire, L., 1965. Palynologie et stratigraphie du Crétacé des bassins du Sénégal et de Côte d'Ivoire. Colloque international de micropaléontologie 32, 187–245.
Kaska, H.V., 1989. A spore and pollen zonation of early cretaceous to tertiary non-marine sediments of central Sudan. Palynology 13, 79–90. https://doi.org/10.1080/01916122.1989.9989356.
Kier, P.M., Lawson, M.H., 1978. Index of living and fossil echinoids 1924–1970. Smithsonian Contributions to Paleobiology 1–182. https://doi.org/10.5479/si.00810266.34.1.
Kolonic, S., Wagner, T., Forster, A., Sinninghe Damsté, J.S., Walsworth-Bell, B., Erba, E., Turgeon, S., Brumsack, H., Chellai, E.H., Tsikos, H., Kuhnt, W., Kuypers, M.M.M., 2005. Black shale deposition on the northwest African Shelf during the Cenomanian/Turonian oceanic anoxic event: climate coupling and global organic carbon burial. Paleoceanography 20. https://doi.org/10.1029/2003PA000950.
Koutsoukos, E.A.M., Leary, P.N., Hart, M.B., 1990. Latest Cenomanian – earliest Turonian low-oxygen tolerant benthonic foraminifera: a case-study from the Sergipe basin (N.E. Brazil) and the western Anglo-Paris basin (southern England). Palaeogeography, Palaeoclimatology, Palaeoecology 77, 145–177. https://doi.org/10.1016/0031-0182(90)90130-Y.
Koutsoukos, E.A.M., Mello, M.R., Azambuja Filho, N.C., 1991. Micropaleontological and geochemical evidence of mid-Cretaceous dysoxic-anoxic paleoenvironments in the Sergipe Basin, northeastern Brazil. In: Tyson, R.V., Pearson, T.H. (Eds.), Modern and Ancient Continental Shelf Anoxia. Geological Society, London, Special Publications, pp. 427–447.
Lapão, L.G.P., Simão, M.V.C., 1973. Carta Geológica de Angola na escal 1/100.000. Folha n^{o} 184 (Novo Redondo). Direcção Provincial dos Serviços de Geologia e Minas, Luanda.
Lister, J.K., Batten, D.J., 1988. Stratigraphic and palaeoenvironmental distribution of Early Cretaceous dinoflagellate cysts in the Hurlands Farm Borehole, West Sussex, England. Palaeontographica Abteilung B Band 210, 9–89.
Magniez-Jannin, F., Muller, C., 1987. Cretaceous stratigraphic and paleoenvironmental data from the South Atlantic (foraminifers and nannoplankton). Revista Brasileira de Geociencias 17, 100–105.
Masure, E., Rauscher, R., Dejax, J., Schuler, M., Ferré, B., 1998. Cretaceous-Paleocene palynology from the Côte d'ivoire-Ghana transform margin. SITES 959, 960–961. AND 962 1, Scientific Results.
Masure, E., Dejax, J., De Ploëg, G., 2013. Blowin' in the wind… 100Ma old multi-staged dinoflagellate with sexual fusion trapped in amber: marine–freshwater transition. Palaeogeography, Palaeoclimatology, Palaeoecology 388, 128–144. https://doi.org/10.1016/j.palaeo.2013.08.008.
Meijer, M., 1989. Au sujet d'une collection de microfossiles d'Angola. (Summa Micropalaeontologiae Angolensis 1953–1983). Musée royal de l'Afrique centrale, pp. 159–164. Rapports annuels 1987–1988.
Mello, M.R., Koutsoukos, E.A.M., Hart, M.B., Brassell, S.C., Maxwell, J.R., 1989. Late cretaceous anoxic events in the Brazilian continental margin. Organic Geochemistry 14, 529–542. https://doi.org/10.1016/0146-6380(89)90033-8.
Morais, M.L., Menardi Noguera, A., Rizzini, A., 1990. Rilievo geologico e strutturale dell'area di Cabo Ledo, con dettagli sedimentologici sulle formazioni Quissonde e Cabo Ledo; bacino del Rio Kwanza, Angola. Atti Ticinensi di Scienze della Terra 33, 109–126.
Moulin, M., Aslanian, D., Unternehr, P., 2010. A new starting point for the South and Equatorial Atlantic Ocean. Earth-Science Reviews 98, 1–37. https://doi.org/10.1016/j.earscirev.2009.08.001.
Mueller, S., Veld, H., Nagy, J., Kürschner, W.M., 2014. Depositional history of the Upper Triassic Kapp Toscana Group on Svalbard, Norway, inferred from palynofacies analysis and organic geochemistry. Sedimentary Geology 310, 16–29. https://doi.org/10.1016/j.sedgeo.2014.06.003.
Néraudeau, D., Mathey, B., 2000. Biogeography and diversity of South Atlantic Cretaceous echinoids: implications for circulation patterns. Palaeogeography, Palaeoclimatology, Palaeoecology 156, 71–88. https://doi.org/10.1016/S0031-0182(99)00132-7.
O'Brien, C.L., Robinson, S.A., Pancost, R.D., Sinninghe Damsté, J.S., Schouten, S., Lunt, D.J., Alsenz, H., Bornemann, A., Bottini, C., Brassell, S.C., Farnsworth, A., Forster, A., Huber, B.T., Inglis, G.N., Jenkyns, H.C., Linnert, C., Littler, K., Markwick, P., McAnena, A., Mutterlose, J., Naafs, B.D.A., Püttmann, W., Sluijs, A., van Helmond, N.A.G.M., Vellekoop, J., Wagner, T., Wrobel, N.E., 2017. Cretaceous sea-surface temperature evolution: constraints from TEX86 and planktonic foraminiferal oxygen isotopes. Earth-Science Reviews 172, 224–247. https://doi.org/10.1016/j.earscirev.2017.07.012.
Quesne, D., Buta-Neto, A., Benard, D., Guiraud, M., 2009. Distribution of Albian clastic deposits in the Benguela basin (Angola): evidence of a Benguela palaeocurrent? Bulletin de la Societe Geologique de France 180, 117–129. https://doi.org/10.2113/gssgfbull.180.2.117.
Regali, M.S.P., Uesugui, N., Santos, A.S., 1974. Palinologia dos sedimentos mesocenozoicos do Brasil (II). Boletim Tecnico da Petrobras 17, 263–301.
Riding, J.B., Warny, S., 2008. Palynological techniques. In: Clair, A., Riding, Brown J.B., Warny, S. (Eds.), American Association of Stratigraphic Palynologists Foundation, second ed., pp. 1–137.
Rodrigues, R., 2005. Chemostratigraphy. In: Koutsoukos, E.A. (Ed.), Applied Stratigraphy. Springer, p. 16.
Schiøler, P., Riding, J.B., Brinkhuis, H., 2012. Late Cretaceous Northern Hemisphere. In: 2012 Utrecht DINOCOURSE Session#7.
Schlanger, S.O., Jenkyns, H.C., 1976a. Cretaceous anoxic events: causes and consequences. Geologie en Mijnbouw 55, 179–184.
Schlanger, S.O., Jenkyns, H.C., 1976b. Cretaceous oceanic anoxic events: causes and consequences. Geologie en Mijnbouw 55, 179–184.
Schlanger, S.O., Arthur, M.A., Jenkyns, H.C., Scholle, P.A., 1987. The Cenomanian-Turonian oceanic anoxic event, I. In: Stratigraphy and Distribution of Organic Carbon-Rich Beds and the Marine δ^{13}C Excursion, vol. 26. Geological Society, London, Special Publications, pp. 371–399. https://doi.org/10.1144/GSL.SP.1987.026.01.24.
Schrank, E., 1990. Palynology of the clastic Cretaceous sediments between Dongola and Wadi Muqaddam, Northern Sudan. Berliner geowissenschaftliche Abhandlungen 120, 149–168.
Schrank, E., 2001. Palaeoecological aspects of Afropollis/Elaterates peaks (Albian-Cenomanian pollen) in the Cretaceous of Northern Sudan and Egypt. In: Goodman, D.K., Clarke, R.T. (Eds.), 11th International Proceedings, Palynological Congress. American Association of Stratigraphers and Palynologists Foundation, pp. 201–210.
Serié, C., Huuse, M., Schødt, N.H., Brooks, J.M., Williams, A., 2017. Subsurface fluid flow in the deep-water Kwanza Basin, offshore Angola. Basin Research 29, 149–179. https://doi.org/10.1111/bre.12169.
Skupien, P., Mohamed, O., 2008. Campanian to Maastrichtian palynofacies and dinoflagellate cysts of the Silesian Unit, Outer Western Carpathians, Czech Republic. Bulletin of Geosciences 207–224. https://doi.org/10.3140/bull.geosci.2008.02.207.
Skupien, P., Vasicek, Z., 2002. Lower Cretaceous Ammonite and Dinocyst biostratigraphy and paleoenvironment of the Silesian Basin (Outer Western Carpathians). Geologica Carpathica 53, 179–189.
Smith, A.G., Smith, D.G., Funnell, B.M., 1994. Atlas of Mesozoic and Cenozoic Coastlines. Cambridge University Press, Cambridge, pp. 1–99.
Srivastava, S.K., 1981. Stratigraphic ranges of selected spores and pollen from the Fredericksburg group (Albian) of the southern United States. Palynology 5, 1–27. https://doi.org/10.1080/01916122.1981.9989215.
Strganac, C., Salminen, J., Jacobs, L.L., Polcyn, M.J., Ferguson, K.M., Mateus, O., Schulp, A.S., Morais, M.L., Tavares, T. da S., Gonçalves, A.O., 2014. Carbon isotope stratigraphy, magnetostratigraphy, and 40Ar/39Ar age of the Cretaceous South Atlantic coast, Namibe Basin, Angola. Journal of African Earth Sciences 99, 452–462. https://doi.org/10.1016/j.jafrearsci.2014.03.003.
Tedeschi, L.R., Jenkyns, H.C., Robinson, S.A., Sanjinés, A.E.S., Viviers, M.C., Quintaes, C.M.S.P., Vazquez, J.C., 2017. New age constraints on Aptian evaporites

and carbonates from the South Atlantic: implications for Oceanic Anoxic Event 1a. Geology 45, 543–546. https://doi.org/10.1130/G38886.1.

Thusu, B., Van Der Eem, J.G.L.A., 1985. Early Cretaceous (Neocomian-Cenomanian) Palynomorphs. Journal of Micropalaeontology 4, 131–149. https://doi.org/10.1144/jm.4.1.131.

Tocher, B.A., Jarvis, I., 1987. Dinoflagellate cysts and stratigraphy of the Turonian (Upper Cretaceous) chalk near Beer, southeast Devon, England. In: Hart, M.B. (Ed.), Micropalaeontology of Carbonate Environments. British Micropalaeontology Society Series Ellis Horwood, Chichester, 198–175.

Total-Sonangol, 1987. Carte Geologique du Bassin du Kwanza, Angola (1:250 000).

Tyson, R.V., 1993. Chapter 5: palynofacies analysis. In: Jenkins, D.G. (Ed.), Applied Micropaleontology. Kluwer Academic Publishers, The Netherlands, Amsterdam, pp. 153–191.

Tyson, R.V., 1995. Sedimentary organic matter. In: Organic Facies and Palynofacies. Chapman & Hall, London, pp. 1–615.

Tyson, R.V., Follows, B., 2000. Palynofacies prediction of distance from sediment source: a case study from the Upper Cretaceous of the Pyrenees. Geology 28, 569. https://doi.org/10.1130/0091-7613(2000)28<569:PPODFS>2.0.CO;2.

Valle, B., Dal' Bó, P.F., Mendes, M., Favoreto, J., Rigueti, A.L., Borghi, L., de Oliveira Mendonça, J., Silva, R., 2019. The expression of the Oceanic Anoxic Event 2 (OAE2) in the northeast of Brazil (Sergipe-Alagoas Basin). Palaeogeography, Palaeoclimatology, Palaeoecology 529, 12–23. https://doi.org/10.1016/j.palaeo.2019.05.029.

Wang, C., Hu, X., Huang, Y., Wagreich, M., Scott, R., Hay, W., 2011. Cretaceous oceanic red beds as possible consequence of oceanic anoxic events. Sedimentary Geology 235, 27–37. https://doi.org/10.1016/j.sedgeo.2010.06.025.

Williams, G., Brinkhuis, H., Pearce, M., Fensome, R., Weegink, J., 2004. Southern Ocean and Global Dinoflagellate Cyst Events Compared: Index Events for the Late Cretaceous-Neogene 1.

Williams, G.L., Fensome, R.A., MacRae, R.A., 2017a. DINOFLAJ3 [WWW Document]. American Association of Stratigraphic Palynologists, Data Series no. 2. http://dinoflaj.smu.ca/dinoflaj3.

Williams, G.L., Fensome, R.A., Macrae, R.A., 2017b. The Lentin and Williams index of fossil Dinoflagellates 2017 edition. American Association of Stratigraphic Palynologists Contributions 48, 1–1097.

Wilpshaar, M., Leereveld, H., 1994. Palaeoenvironmental change in the Early Cretaceous Vocontian Basin (SE France) reflected by dinoflagellate cysts. Review of Palaeobotany and Palynology 84, 121–128. https://doi.org/10.1016/0034-6667(94)90046-9.

Wood, G.D., Gabriel, A.M., Lawson, J.C., 1996. Palynological techniques-processing and microscopy. In: Jansonius, J., Mcgregor, D.C. (Eds.), Palynology: Principles and applications, vol. 1. American Association of Stratigraphic Palynologists, pp. 29–50.

Zobaa, M.K., Oboh-Ikuenobe, F.E., Ibrahim, M.I., 2011a. The Cenomanian/Turonian oceanic anoxic event in the Razzak Field, north Western Desert, Egypt: Source rock potential and paleoenvironmental association. Marine and Petroleum Geology 28, 1475–1482. https://doi.org/10.1016/j.marpetgeo.2011.05.005.

Zobaa, M.K., Zavada, M.S., Whitelaw, M.J., Shunk, A.J., Oboh-Ikuenobe, F.E., 2011b. Palynology and palynofacies analyses of the Gray Fossil Site, eastern Tennessee: their role in understanding the basin-fill history. Palaeogeography, Palaeoclimatology, Palaeoecology 308, 433–444. https://doi.org/10.1016/j.palaeo.2011.05.051.

Zobaa, M.K., El Beialy, S.Y., El-Sheikh, H.A., El Beshtawy, M.K., 2013. Jurassic–Cretaceous palynomorphs, palynofacies, and petroleum potential of the Sharib-1X and Ghoroud-1X wells, north Western Desert, Egypt. Journal of African Earth Sciences 78, 51–65. https://doi.org/10.1016/j.jafrearsci.2012.09.010.

Appendix A. Supplementary data

Supplementary data to this article can be found online at https://doi.org/10.1016/j.cretres.2024.105953.